



OPEN ACCESS

EDITED BY

Isabelle Mack,
University of Tübingen, Germany

REVIEWED BY

Imad Al Kassaa,
Fonterra (New Zealand), New Zealand
Zhaocheng Ma,
Huazhong Agricultural University, China

*CORRESPONDENCE

Meng-Liang Tian

✉ secondat@sicau.edu.cn

[†]These authors have contributed equally to this work

SPECIALTY SECTION

This article was submitted to
Nutritional Immunology,
a section of the journal
Frontiers in Immunology

RECEIVED 05 February 2023

ACCEPTED 31 March 2023

PUBLISHED 21 April 2023

CITATION

Zou Y-F, JiZe X-P, Li C-Y, Zhang C-W,
Fu Y-P, Yin Z-Q, Li Y-P, Song X, Li L-X,
Zhao X-H, Feng B, Huang C, Ye G,
Tang H-Q, Li N-Y, Chen J, Chen X-F and
Tian M-L (2023) Polysaccharide from aerial
part of *Chuanminshen violaceum* alleviates
oxidative stress and inflammatory response
in aging mice through modulating
intestinal microbiota.
Front. Immunol. 14:1159291.
doi: 10.3389/fimmu.2023.1159291

COPYRIGHT

© 2023 Zou, JiZe, Li, Zhang, Fu, Yin, Li, Song,
Li, Zhao, Feng, Huang, Ye, Tang, Li, Chen,
Chen and Tian. This is an open-access article
distributed under the terms of the [Creative
Commons Attribution License \(CC BY\)](#). The
use, distribution or reproduction in other
forums is permitted, provided the original
author(s) and the copyright owner(s) are
credited and that the original publication in
this journal is cited, in accordance with
accepted academic practice. No use,
distribution or reproduction is permitted
which does not comply with these terms.

Polysaccharide from aerial part of *Chuanminshen violaceum* alleviates oxidative stress and inflammatory response in aging mice through modulating intestinal microbiota

Yuan-Feng Zou^{1,2†}, Xiao-Ping JiZe^{1†}, Cen-Yu Li¹,
Chao-Wen Zhang¹, Yu-Ping Fu¹, Zhong-Qiong Yin¹,
Yang-Ping Li³, Xu Song¹, Li-Xia Li¹, Xing-Hong Zhao¹,
Bin Feng⁴, Chao Huang², Gang Ye¹, Hua-Qiao Tang¹,
Ning-Yuan Li¹, Ji Chen⁵, Xing-Fu Chen⁵ and Meng-Liang Tian^{5*}

¹Natural Medicine Research Center, College of Veterinary Medicine, Sichuan Agricultural University, Chengdu, China, ²Key Laboratory of Animal Disease and Human Health of Sichuan Province, College of Veterinary Medicine, Sichuan Agricultural University, Chengdu, China, ³State Key Laboratory of Crop Gene Exploration and Utilization in Southwest China, Chengdu, China College of Agronomy, Sichuan Agricultural University, Chengdu, China, ⁴Animal Nutrition Institute, Sichuan Agricultural University, Chengdu, China, ⁵College of Agronomy, Sichuan Agricultural University, Chengdu, China

Aging is a biological process of progressive deterioration of physiological functions, which poses a serious threat to individual health and a heavy burden on public health systems. As population aging continues, research into anti-aging drugs that prolong life and improve health is of particular importance. In this study, the polysaccharide from stems and leaves of *Chuanminshen violaceum* was obtained with water extraction and alcohol precipitation, and then separated and purified with DEAE anion exchange chromatography and gel filtration to obtain CVP-AP-I. We gavaged natural aging mice with CVP-AP-I and performed serum biochemical analysis, histological staining, quantitative real-time PCR (qRT-PCR) and ELISA kit assays to analyze inflammation and oxidative stress-related gene and protein expression in tissues, and 16SrRNA to analyze intestinal flora. We found that CVP-AP-I significantly improved oxidative stress and inflammatory responses of the intestine and liver, restored the intestinal immune barrier, and balanced the dysbiosis of intestinal flora. In addition, we revealed the potential mechanism behind CVP-AP-I to improve intestinal and liver function by regulating intestinal flora balance and repairing the intestinal immune barrier to regulate the intestinal-liver axis. Our results indicated that *C. violaceum* polysaccharides possessed favorable antioxidant, anti-inflammatory and potentially anti-aging effects *in vivo*.

KEYWORDS

Chuanminshen violaceum, polysaccharide, antioxidation, antiinflammatory, gut-liver axis, gut microbiota

1 Introduction

Aging is a process of deterioration of the body's tissues and organs over time, with a decline in the function of all systems, eventually leading to cellular and even individual death. With age-related diseases such as Alzheimer's disease, Parkinson's disease, cardiovascular disease as well as cancer increasing exponentially worldwide in recent years (1–3), there is a constant desire to slow or even reverse aging. Aging is a multifaceted biological process resulted from the combined effect of many factors, and the most widely accepted theory of aging is the free radical theory of aging (4). The free radical theory suggests that increased oxidative stress is an important driver of aging. Under normal physiological conditions, redox levels remain in balance. As we age, the body produces more free radicals (mainly ROS), but the reduced activity of enzymes involved in scavenging free radicals leads to oxidative stress damage (5, 6) and chronic inflammation (7, 8), thus exhibiting the characteristics of aging. One of the main features of aging is the decline in intestinal digestive functions, manifested by disturbances in the intestinal flora, atrophy of the intestinal mucosa and destruction of intestinal immune function (9, 10). This intestinal dysfunction allows microorganisms (or derived metabolites) and toxins (LPS) to enter the circulation and reach the liver, causing or worsening a range of liver diseases (11, 12). Similarly, aging-induced decreases in the metabolic and detoxification functions of the liver affect the intestinal tract through bile acids (13, 14). This bidirectional relationship between the gut and liver *via* the portal vein, known as the gut-liver axis, was first proposed in 1988 and has attracted widespread attention (15). Accumulated studies show that liver and intestinal diseases can be treated through the gut-liver axis theory (16, 17), which shows that the gut-liver axis balance is so important for a healthy body. The gut microbes, which are part of this two-way communication between the gut and liver, are essential for maintaining the homeostasis of the gut-liver axis (18, 19). In recent years, there has been an increasing amount of research into the use of microbiota-targeted dietary and probiotic interventions and novel therapeutic applications such as faecal microbiota transplantation in the prevention and treatment of ageing-related diseases (20). Therefore, screening and identifying potential therapeutic molecules that balance the gut microflora against aging is of great significance.

Chuanminshen violaceum Sheh et Shan (CVSS), mainly distributed in Sichuan and Hubei provinces, traditionally used as a medicine from the roots, it is both a bulk Chinese herb and a premium nutritional health product, mostly used as a fitness tonic and as an edible ingredient in folklore for hundreds of years (21). Natural polysaccharides have attracted great interest due to their wide range of sources, low toxicity, few side effects and diverse biological activities (22). Pharmacological studies have shown that polysaccharides are the main active ingredients of CVSS and have various activities such as antioxidant (23), immunomodulatory (24) and antiviral (25). In the industrial production of traditional Chinese medicine, non-medicinal parts, such as stems and leaves of traditional root-based medicines, are generally discarded, resulting in a waste of resources and environmental pollution.

These plant parts may be suitable plant resources for the production of phytochemicals (26). Numerous studies have shown that non-medicinal parts of traditional Chinese herbs have the same biological activity as their medicinal counterparts (27, 28). Therefore, in this study, we aimed to evaluate whether CVSS polysaccharide can alleviate oxidative stress injury and inflammatory response in the gut and liver of naturally aging mice, and to investigate the potential function of CVSS polysaccharide in the gut-liver axis and their correlation with gut microbiota to provide evidence for the further development and utilization of CVSS.

2 Materials and methods

2.1 Materials

The stems and leaves of *Chuanminshen violaceum* were collected from Bazhong City, Sichuan Province, in April 2022 and identified by Dr Yuan-Feng Zou, College of Veterinary Medicine, Sichuan Agricultural University. The fresh stem leaves are treated in an oven at 105°C for 15 minutes to destroy and blunt the oxidase activity in the leaves by high temperature, inhibit the enzymatic oxidation of tea polyphenols etc. in the fresh leaves and evaporate some of the water in the fresh leaves, then dried at 55°C to constant weight and sheared into flakes then dried at 55°C to constant weight and sheared into pieces

2.2 Isolation, chemical composition, monosaccharide composition and average-molecular weight of CVSS polysaccharides

The extraction of polysaccharides was carried out based on the previous method (29). Briefly, the dried stems and leaves of *Chuanminshen violaceum* (100g) were pre-treated by 90% ethanol (v/v) to remove impurities until colorless, then the dried residues were treated with boiling water under the following conditions: 100°C, 2 h, solid-liquid ratio 1:20, 2 times. The extract was extracted by filtration, alcohol precipitation, dialysis (cut off 3500 Da) and loaded to a lyophilizer (LGJ-10G, Beijing Sihuan Qihang technology Co., Ltd., Beijing, China) to obtain CVSS crude polysaccharide (CVP) powder. For further purification, CVP (400 mg) was dissolved in distilled water (20 mL), centrifuged, filtrated (0.45 µm) and applied into an anion-exchange column packed with DEAE-Sephacrose Fast Flow (50 mm × 40 cm; Beijing Rui Da Heng Hui Science Technology Development Co., Ltd, Beijing, China). The neutral and acidic fractions were eluted with 2 L distilled water followed by 0–1.5 mol/L NaCl solution at a flow rate of 2 mL/min, respectively. The elution profiles of acidic fractions were monitored by the phenol-sulfuric acid method (30), and the acid polysaccharide fraction was collected according to the elution profiles, followed by dialysis (cut off 3500 Da) to remove NaCl, concentrating and freeze-drying, named as CVP-AP. Finally, CVP-AP was further purified by gel filtration (Sephacrose 6FF, 2.5 cm ×

100 cm, Beijing Rui Da Heng Hui Science Technology Development Co. Ltd) to obtain a purified fraction (31), named CVP-AP-1, because it was more purified than CVP-AP, CVP-AP-I was collected and lyophilized for subsequent studies.

The total carbohydrate content of CVP-AP-I was determined by the phenol sulfuric acid method (30), the total amounts of phenolic compounds and proteins of CVP-AP-I were determined by Folin-Ciocalteu (32) and Bio-Rad protein assay (33). Referring to previous research methods (34), the monosaccharide composition of CVP-AP-I was determined by HPLC (Agilent Technologies, 1260 Infinity II, USA). Briefly, CVP-AP-I was dissolved in TFA (trifluoroacetic acid) and then hydrolyzed at 100°C for 8 h. After repeated evaporation and concentration with methanol to remove excess TFA, the sample was then derivatized with NaOH and PMP (1-phenyl-3-methyl-5-pyrazolone)-methanol at 70°C for 100 min, and finally the pH was adjusted to neutral and extracted with chloroform to obtain the sample derivative. The standard monosaccharide mix including mannose (Man), ribose (Rib), Rhamnose (Rha), glucuronic acid (GlcA), galacturonic acid (GalA), glucose (Glc), galacturonic (Gal), xylose (Xyl) and arabinose (Ara) were derivatized at the same manner. All derivatives were chromatographed on HPLC equipped with C18 column (250 nm × 4.6 mm, 5 μm), with following settings: mobile phase: 0.05 mol/L phosphate buffer (NaH₂PO₄-Na₂HPO₄, pH6.8)-acetonitrile (82:18, V/V); flow rate: 1.0 mL/min; column temperature 30°C; detection wavelength of DAD was 250 nm; injection volume: 20 μL.

The molecular weight (Mw) of CVP-AP-I was determined by gel permeation chromatography method (Waters 515 liquid chromatography pump, Waters 2410 differential detector (Refractive Index), Waters Ultrahydrgel Linear gel column (300 × 7.8 mm) (34, 35). The Mw control dextran (2.5–5348 Da) and CVP-AP-I were dissolved in the mobile phase. Sample solutions were injected after the system was stable, and the resulting chromatogram was recorded. The weight-average molecular weight (Mw), number-average molecular weight (Mn) and their distribution equivalents

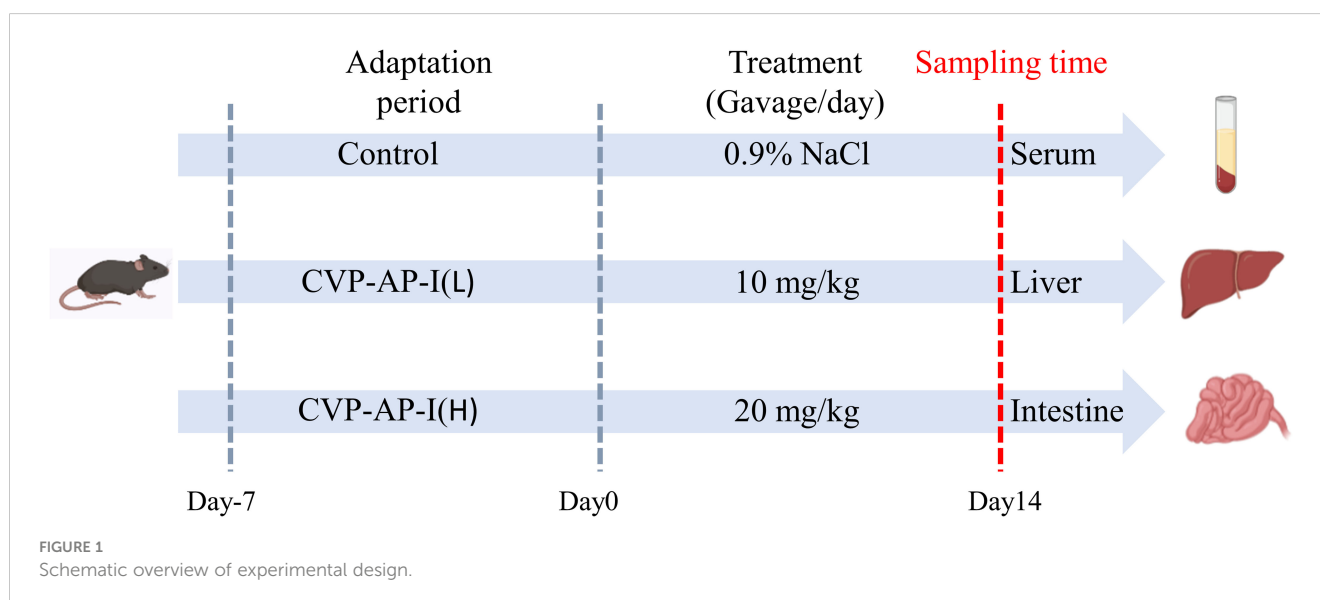
were obtained by the standard curve. The chromatographic conditions are as follows: the mobile phase was 0.2 mol/L NaNO₃ solution, pH = 6.0; flow rate was 0.6 mL/min; the column temperature: 40°C; the injection volume was 20 μL.

2.3 Animal care and experimental design

All animal studies were conducted in accordance with the Animal Care and Use Committee guidelines of Sichuan Agricultural University. Thirty male specific-pathogen-free C57BL/6 mice (48 weeks old) were purchased from Beijing Vital River Laboratory Animal Technology Co., Ltd (Beijing China), and housed in a pathogen free environment and free access to standard chow and water for 7 days, with an automatically controlled 12 h light/dark cycle, the temperature was 25 ± 2°C and the humidity was 60%. After the acclimatization period, as shown in Figure 1, all mice were randomly divided into three groups (10 mice in each group), and received a daily gavage of solution (same volume of saline), 10 mg/kg polysaccharide, or 20 mg/kg polysaccharide group for 14 consecutive days. Food intake was recorded daily and body weight was measured every 2 days. At the end of the experiment, all mice were fasted overnight, blood was collected from the eyeballs the next day. Finally, they were euthanized and dissected quickly, then the main organs of liver, intestine tissue, and cecum contents were collected rapidly. All tissue samples were divided into two parts, one was frozen in liquid nitrogen, and then stored at -80 °C for gene expression analysis and biochemical analysis, the other one was fixed in 4% paraformaldehyde for subsequent histopathological examination.

2.3.1 Blood biochemical test

The biochemical indexes of serum, including alanine aminotransferase (ALT), aspartic aminotransferase (AST), triglyceride (TG) and total cholesterol (TC), were detected by automatic hematology analyzer (Shenzhen Icbio Biomedical Technology Co., Ltd.).



2.3.2 Histological staining

The duodenum, jejunum, ileum and liver tissue fixed in 4% paraformaldehyde solution were cut into appropriate size. The tissues were embedded in paraffin and cut into 5µm sections, then stained with hematoxylin and eosin according to the manufacturer's instructions (H&E, G1260, Solarbio, Beijing, China). Brightfield images at 200 × magnification were captured on Nikon Eclipse Ti microscope (Melville, NY, USA).

2.3.3 Quantitative realtime PCR

The intestine (duodenum, jejunum, ileum) and liver tissues were ground under liquid nitrogen. The total RNA was extracted with TRIzol reagent (Biomed, Beijing, China) from the tissue powder, then the RNA (5 µg/µL) was reverse transcribed into cDNA using M-MLV 4 First-Strand cDNA Synthesis Kit (Biomed, RA101-12, China) and further applied to qRT-PCR in a step Oneplus System (Biosystems, Foster City, CA, USA) using determine double-stranded DNA. The procedure conditions were one cycle of 30s at 95°C for pre-denaturation, 40 cycles of 95°C (10 s) and optimum annealing temperature (30s) for denaturation and annealing/extension, respectively. The gene expression levels were calculated according to the regulative relevant quantification method followed by the $\Delta\Delta CT$ method (34). The relative gene expression was normalized to internal control as β -Actin. The primer sequences (Tsingke Biotechnology Co., Ltd, China) for genes expression detection in this study are listed in Table 1.

2.3.4 Determination of oxidative stress indicators, inflammatory factors, LPS and sIgA

The concentrations of inflammatory factors (IL-6, IL-1 β , TNF- α) and LPS in serum, liver and jejunum, and sIgA in jejunum were determined by ELISA kits according to the manufacturer's instructions (MIBio, Shanghai, China). The levels of SOD (superoxide dismutase), CAT (catalase), GPX (glutathione peroxidase) and MDA (malondialdehyde) in serum, jejunum and liver tissues, as well as ROS (reactive oxygen species) and T-AOC (total antioxidant capacity) levels in tissues were analyzed with biochemical kits according to the manufacturer's instructions (Nanjing Jiancheng Biotechnology Institute, China). the total protein concentration was assessed according to the BCA assay kit (Beyotime, Shanghai, China).

2.3.5 Gut microbiota analysis

Fresh digesta isolated from the cecum was quickly sent to Novogene Technology Co., Ltd. (Beijing, China), under dry ice conditions for gut microbiota analysis. The DNA was extracted using CTAB/SDS (cetyltrimethylammonium bromide/sodium dodecyl sulfate) Bromide method, and diluted to 1 ng/µL using sterile water. The V4 region of 16S rRNA was amplified by PCR using specific primers (515F: CCTAYGGGRBGCASCAG; 806R: GGACTACNNGGGTATCTAAT), followed by mixing and purification of PCR products, and library construction using TruSeq[®] DNA PCR-Free Sample Preparation Kit. The libraries were quantified by Qubit and Q-PCR, and then sequenced using NovaSeq 6000.

TABLE 1 primer sequences for qRT-PCR.

Gene	Primer sequence 5' to 3'	PubMed no.	bp
β -actin	F: TCACGGTTGGCCTTAGGGTTC R: CGCTCGTTGCCAATAGTG	NM_001259638.1	71
IL-1 β	F: CCTGTGTTTTCTCCTTGCCCT R: AGTGCGGGCTATGACCAATTC	NM_008361.4	158
TNF- α	F:CTCTTCTCATTCTGCTCGT R: ACCCCGAAGTTCAGTAGACA	NM_012675.3	62
IL-6	F: AAATATGAGACTGGGGATGTC R: TCAGTCCCAAGAAGGCAAC	NM_001314054	90
CAT	F: ACCAGATACTCCAAGGCAAA R: TAAAATTTCACTGCAAACCCC	NM_009804.2	137
SOD1	F: GAACCATCCACTTCGAGCAG R: ATCACACGATCTTCAATGGAC	NM_011434.2	265
GPX	F: TGCTTGCTCCTAAATGCTG R: CCCAGAATGACCAAGCCAA	NM_001329860.1	81
Nrf2	F: AACCTCCCTGTTGATGACTTC R: CTGTCTGTTTTCTCCCTTTTCTC	NM_001399226.1	76
Muc2	F: TCATCAACCTTCACTACCCCA R: TTTTGACACTAACCCAAAC	NM_023566.4	247
ZO-1	F: TCGATCAAATCATTACGACCCT R: GCTCTCAAACCTTCTTCGGTCAA	NM_001352638.1	55
Occludin	F: TTGAAAAGTCCACCTCCTTACAGA R: CCGGATAAAAAGAGTACGCTGG	NM_001360536.1	129

2.4 Statistical analysis

Data represent the mean \pm standard deviation (SD) or mean \pm standard error of the mean (SEM). One-way ANOVA with LSD *post-hoc* test was performed by using SPSS 27.0 software. The *p*-value of 0.05 or less was considered with statistically significance.

3 Results

3.1 Isolation, chemical composition, monosaccharide composition and average-molecular weight of CVSS polysaccharide

Crude polysaccharide (CVP) was obtained from the stems and leaves of CVSS by water extraction and alcohol precipitation, with a yield of 5.06%. There are no previous reports related to polysaccharides from the stems and leaves of CVSS, but the extraction rates of crude polysaccharides from CVSS leaves were reported to be in the range of 4.73%–5.41% (36), which were similar to our extraction rates. CVP was separated by DEAE anion exchange chromatography to obtain an acidic component CVP-AP (Figure 2A), but the neutral component isolation was less than 1%, so it was not included in the follow-up study. CVP-AP was further purified by gel filtration to obtain CVP-AP-I with a yield of 81.93% (Figure 2B). The monosaccharide composition of CVP-AP-I was determined by HPLC and the results (Figure 2C) showed that the monosaccharides present in CVP-AP-I were mainly galacturonic acid (GalA), galactose (Gal), arabinose (Ara), rhamnose (Rha), and a small amount of mannose (Man). The

total carbohydrate content of the CVP-AP-I was 89.91%, the total protein was 4.51%, and the total polyphenol content was 0.98% (Figure 2C). Compared with the reported polysaccharides from the roots and leaves of CVSS, the monosaccharide types and molar ratios of CVP-AP-I were different (36, 37). The weight-average molecular weight (Mw) of CVP-AP-I was 118.2 kDa, as determined by gel permeation chromatography, and a single symmetric peak was observed, as shown in Figure 2D.

3.2 CVP-AP-I protects naturally aging mice from oxidative stress and inflammation

As we all know, aging is the inevitable process of life. It is characterized by progressive irreversible degenerative changes in the structure and function of the organs with age, under the influence of multiple factors, accompanied by oxidative stress and inflammatory reactions (7, 8, 38, 39). Therefore, drugs that reduce oxidative damage are the first choice for anti-aging. A mouse's life cycle is typically 18 ~ 24 months, with aging-related biomarkers slowly appearing in mice from the 10th month onwards. The mice used in the experiments were nearly 12 months of age, when most of the biomarkers had already started to show changes. Therefore, we used naturally aging mice as a model to study the roles of the CVP-AP-I in the natural aging process of the organism. After two weeks of polysaccharide intragastric administration, the body weight of mice in the polysaccharide group was greater than that in the control group (Figure 3A). Finally, there was a significant increase in body weight in the 20mg/kg polysaccharide group, and no difference in food intake was observed between the three groups. In addition, in the aging process, the activities of liver function

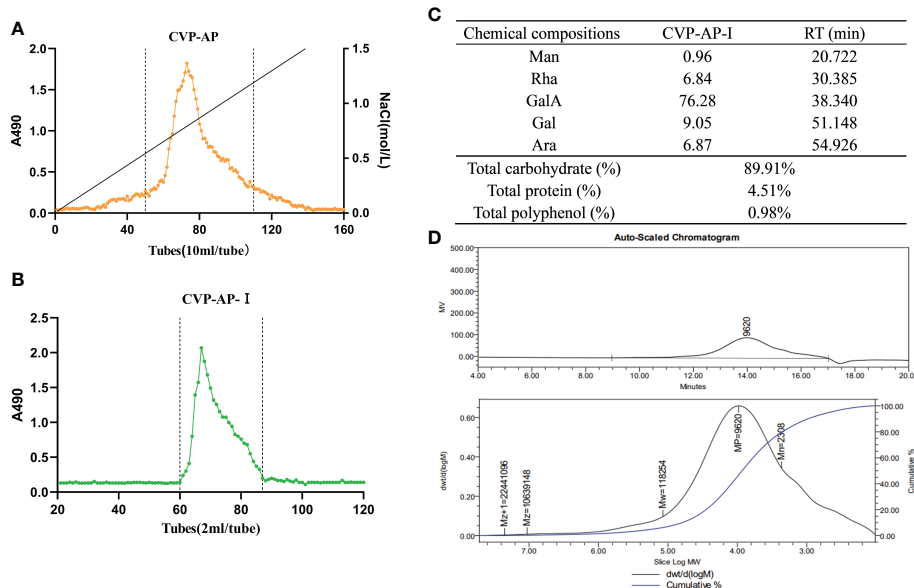


FIGURE 2

Isolation, chemical composition, monosaccharide composition and average-molecular weight of CVSS polysaccharides. (A) The elution curve of CVP-AP on DEAE anion exchange chromatography. A single component is obtained. (B) CVP-AP-I elution profile was obtained after gel filtration purification. (C) The chemical compositions of CVP-AP-I including monosaccharide composition (mol %), total carbohydrate (%), protein content (%), polyphenol content (%). (D) The molecular weight determination of CVSS polysaccharide by gel permeation chromatography.

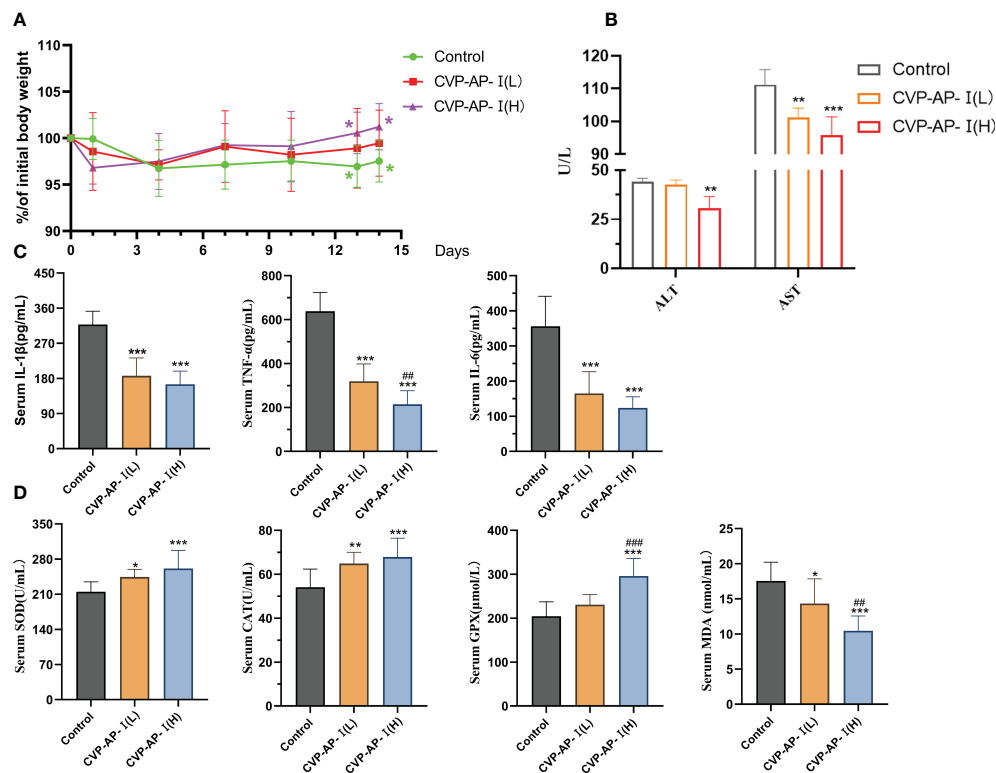


FIGURE 3

Effects of CVP-AP-I on body weight and serum levels of ALT, AST, pro-inflammatory factors (IL-6, IL-1 β , TNF- α), antioxidant enzymes (SOD, CAT, GPX) and MDA in aging mice. (A) Changes in body weight of mice (Relative to initial body weight; n=10); (B) Quantification shows the serum levels of ALT and AST in the mice of different groups (n=4); (C) Quantification shows the inflammatory factor IL-1, TNF- α , IL-6 level in the serum from different groups mice (n=6). (D) Quantification shows the activity of the antioxidant enzymes SOD, CAT and GPX and the level of MDA in the serum of the mice in the different groups (n=6). All data are represented as means \pm SD. * p <0.05, ** p <0.01, and *** p <0.001 as compared with Control Group. ## p <0.01 and ### p <0.001 as compared with CVP-AP-I (L) group.

indicators ALT and AST will continue to rise with the decline of liver function (40). We quantified the activities of ALT and AST in serum, and found that the activities of ALT and AST significantly decreased in polysaccharide group, especially in CVP-AP-I(H) group (Figure 3B). In order to further illustrate the effect of CVSS polysaccharides on aging mice, the serum indicators of inflammation and oxidative stress were quantitatively analyzed. Compared with the aging group, the levels of inflammatory factors IL-1 β , TNF- α and IL-6 (Figure 3C) and MDA in serum (Figure 3D), significantly decreased in the polysaccharide treatment group, while the activities of antioxidant enzymes SOD, CAT and GPX in serum significantly increased (Figure 3D). Previous studies on anti-aging drugs mainly focused on their antioxidant activity, such as astragalus polysaccharide inhibiting D-galactose-induced oxidative stress in mice by upregulating antioxidant factors (41). Inflammation induced by oxidative stress is also another characteristic change of aging. CVSS polysaccharide not only up-regulated serum levels of antioxidant factors but also down-regulated levels of inflammatory factors. All these data indicated that different doses of CVSS polysaccharide interventions in naturally aging mice exhibited great antioxidant activity and anti-inflammatory activity, and may had some ameliorative effects on liver function.

3.3 CVP-AP-I attenuates oxidative stress and inflammation in the gut and liver of naturally aging mice

Systemic chronic inflammatory responses and oxidative stress are the main features of aging, with a decline in intestinal digestive function, which in turn affects the function of other organ tissues (42). Although, CVP-AP-I could significantly reduce the levels of serum inflammatory factors and liver function indicators ALT and AST, and significantly increase the activity of serum antioxidant enzymes. However, polysaccharides as macromolecules may mainly relay on its indirect effect to liver and the intestine, as reported by our group and other researchers (43, 44). Therefore, we further evaluated the effect of CVP-AP-I on antioxidant and anti-inflammatory capacity of gut and liver in naturally aging mice. We observed a decrease trend in the expression of pro-inflammatory genes (IL-1 β , TNF- α and IL-6) and an increase trend in the gene expression of antioxidant enzyme (SOD, CAT and GPX) in the liver, duodenum, jejunum and ileum of aging mice in the polysaccharide-treated groups (Figures 4A, B). Nrf2, an important transcription factor that widely exists in various organs of the body, is considered to be a key transcription factor in regulating cells against xenobiotics and oxidative damage (45, 46);

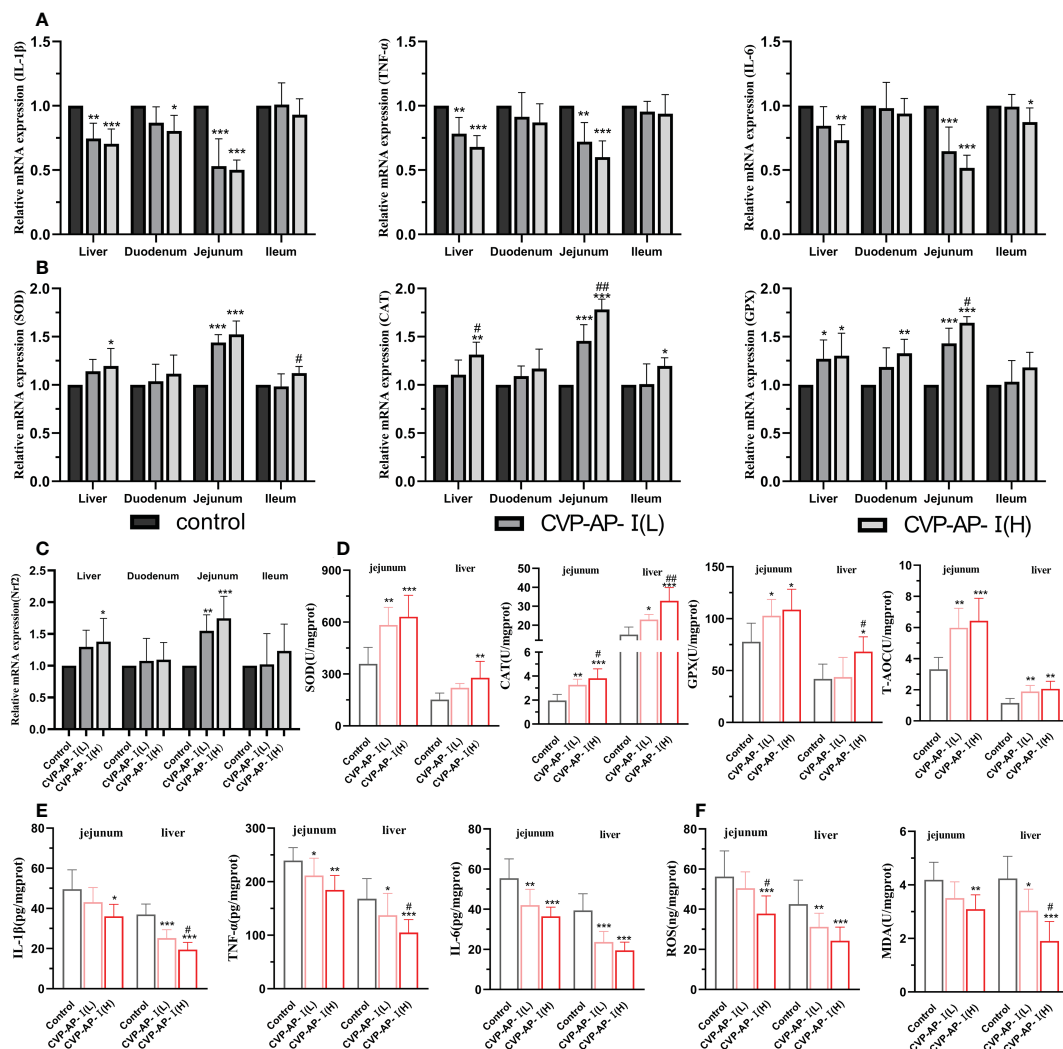


FIGURE 4

Effects of CVP-AP-I on antioxidant and anti-inflammatory capacity of intestine and liver in naturally aging mice. (A) qRT-PCR results show the relative expression levels of inflammatory factors IL-1 β , TNF- α and IL-6 genes in liver and intestinal tissues (duodenum, jejunum and ileum) of different groups of mice (n=5); (B) qRT-PCR results show the relative expression levels of the antioxidant enzymes SOD, CAT and GPX genes in liver and intestinal tissues (duodenum, jejunum and ileum) of different groups of mice (n=5); (C) qRT-PCR results show the relative expression levels of transcription factor Nrf2 gene in liver and intestinal tissues (duodenum, jejunum and ileum) of different groups of mice (n=5); (D) Quantitative results show the protein expression levels of antioxidant enzymes SOD, CAT, GPX and T-AOC in jejunum and liver of mice in different groups (n=6); (E) Quantitative results show the protein expression levels of inflammatory factors IL-1 β , TNF and IL-6 in jejunum and liver of mice in different groups (n=6); (F) Quantitative results show the protein expression of ROS and MDA in jejunum and liver of mice in each group (n=6); All data are represented as means \pm SD. * p <0.05, ** p <0.01, and *** p <0.001 as compared with Control Group. # p <0.05 and ## p <0.01 as compared with CVP-AP-I (L) group.

and on the other hand, scholars have found that Nrf2 also plays a key role in inflammatory repair (47, 48). Polysaccharides have been shown to reduce oxidative stress and inflammatory responses by activating Nrf2 (49, 50). We found that the relative expression of the Nrf2 gene was significantly higher in the jejunum and liver of the CVSS polysaccharide group (Figure 4C), and that the increased expression of antioxidant enzymes and reduced pro-inflammatory factors could be associated with the increase in Nrf2. Although there was a tendency for the polysaccharide-treated groups to alleviate aging-induced oxidative stress and inflammation in the duodenum and ileum, the effect was not significant, so we speculated that the site of utilization of CVSS polysaccharides in the small intestine was primarily in the jejunum. To further illustrate the anti-

inflammatory and antioxidant effects of CVP-AP-I, we then quantified the protein levels of inflammatory factors and antioxidant enzymes in jejunum and liver. As shown in (Figures 4D, E), at the protein level, compared with the control group, CVP-AP-I significantly increased the activities of antioxidant enzymes (SOD, CAT, GPX) and T-AOC in jejunum and liver, and significantly decreased proinflammatory factors (IL-1 β , TNF- α , IL-6) levels, which was consistent with the qRT-PCR results. Finally, we quantified ROS and MDA protein levels in the jejunum and liver. Specific increases of ROS level have been demonstrated as potentially critical for induction and maintenance of cell senescence process (51, 52). And the MDA content is an important parameter reflecting the body's potential

antioxidant capacity, which can amplify the effect of reactive oxygen species and can reflect the rate and intensity of lipid peroxidation in the body, as well as indirectly reflecting the degree of tissue peroxidative damage (53). Additionally, we found that ROS and MDA were significantly lower in the jejunum and liver of the polysaccharide-treated group compared to the control group, and showed a polysaccharide concentration dependence (Figure 4F). These data collectively show the benefits of the CVSS polysaccharide in improving oxidative stress and inflammatory responses in the gut-liver axis of aging mice.

3.4 CVP-AP-I ameliorates liver and intestinal tissue defects and repairs the intestinal immune barrier of naturally aging mice

Our experimental results show that CVP-AP-I not only alleviates intestinal inflammation and oxidative stress, but also has a similar effect on the liver. While the target organ of polysaccharides is the intestine, the intestinal microbiota, intestinal immune response and intestinal permeability are also related to the function of polysaccharides (54). The intestinal tract has been considered an important target organ mediating the body's lifespan extension due to its immune and nutritional intake functions. The decline of digestive and absorption functions in the elderly is caused by histological degeneration of the gastrointestinal tract (55), so we speculate that the protective effects of CVP-AP-I on the gut and liver are mediated through the gut-liver axis. To confirm this speculation at the histopathological level, we first performed H.E staining of the liver and intestine. Subsequently, we found that the livers of aging control mice were structurally disorganized and showed aging features, with inflammatory necrosis of hepatocytes, multinucleated cells and mild steatosis. In contrast, the hepatocytes of the two groups supplemented with CVSS polysaccharide, especially the high-dose group, were neatly arranged in a cord-like arrangement with clear hepatic sinusoidal structures (Figure 5A). In many previous studies, triglyceride (TG) and cholesterol (TC) metabolism disorders and accumulation have been reported to be closely related to aging (56, 57). For example, increased ROS during aging has been reported to play an important role in the accumulation of cholesterol in the liver by increasing cholesterol and glucose uptake to increase cholesterol synthesis (58). Given the previous improvement in hepatocyte steatosis by CVP-AP-I, we subsequently quantified TG and TC in serum, and found that the CVP-AP-I(H) group similarly reduced serum levels of TG and TC (Figure 5E), which was consistent with the results of hepatic H.E staining. In the intestinal tissues, we noted significant histopathological structural defects in the duodenum, jejunum and ileum of the control mice, including fewer and wide villus and reduced number and depth of crypt. Unsurprisingly, we found that the histopathological structure of the intestine (duodenum, jejunum and ileum) of mice supplemented with polysaccharides was more normal, especially in the jejunum of the CVP-AP-I(H) group (Figures 5B–D, F–H).

The small intestinal epithelium is composed of a single layer of cells, associated with each other by tight junctions, and a mucus layer that protects the intestinal epithelial cells surface (59). In

physiological situations, it carries out the exchange and transfer of nutrients and acts as a physical barrier, together with intestinal microorganisms and the host immune system, to maintain intestinal homeostasis (60). Therefore, tight junctions mediated by the integral membrane proteins, peripheral membrane proteins and mucoprotein are essential for the function of the intestinal epithelial barrier, and their defects lead to impaired intestinal permeability and possible translocation of toxic compounds or pathogenic bacteria within the lumen, causing further local or systemic inflammation and many human diseases (61, 62). Intestinal barrier function decreases with age (63, 64), with qRT-PCR results we found that the gene expression of integral membrane protein (Occludin), peripheral membrane protein (ZO-1), and mucoprotein (Muc2) were all elevated in the small intestine of mice in the polysaccharide consumption group (Figure 5I), indicating that CVP-AP-I had an ameliorative effect on intestinal permeability in aging mice. Consistent with this, we detected that CVP-AP-I decreased LPS content in serum and liver (Figure 5J), and promoted the production of sIgA (Figure 5K), a basic and essential enteroendocrine immune antibody. These results suggest that CVSS polysaccharides can improve intestinal and hepatic structural defects and promote the development of the intestinal mucosal immune system.

3.5 CVP-AP-I regulates gut–liver axis through modulating gut microbiota

Intestinal microbial-host interactions are critical in the development and maintenance of body immunity (65). During aging, oxidative stress affects the living environment of intestinal microbes and disrupts the structure and function of intestinal flora, leading to the dysregulation of intestinal flora, and further exacerbates oxidative damage and lipid metabolism disorders (66), thereby aggravating the morbidity and mortality of various chronic diseases. Accumulated studies show that anti-aging can be achieved by regulating the structure and composition of intestinal microbiota (67, 68). As CVSS polysaccharides are not directly available to the organism as macromolecules, we evaluated whether the gut flora was its target and assessed the composition of the gut flora by sequencing the 16S rRNA V4 region of the gut bacteria. The previous data showed that the high-dose polysaccharide administration group had the best anti-aging effect, so the intestinal flora analysis was conducted only for the control group and the high-dose group (named CVP group). As shown in Figure 6A, we first calculated the sample Rarefaction Curves, where the gradual flattening of the curves indicated a reasonable amount of sequencing data and indirectly reflected differences in the abundance of species in different groups respectively (69). Venn diagram analysis revealed 3825 and 1709 OTUs each in the control and CVP groups, with their respective unique OTUs numbers being 2538 and 422, indicating differences in the structure of the gut microflora between the two groups (Figure 6B). Then, we calculated the Chao1 and Shannon indices (70) to assess the richness and diversity of the gut microbiota, and found that they both decreased in the CVP group and Chao1 significantly decreased (Figures 6C, D). To determine the differences in gut microbiota structure between the different groups, Unifrac

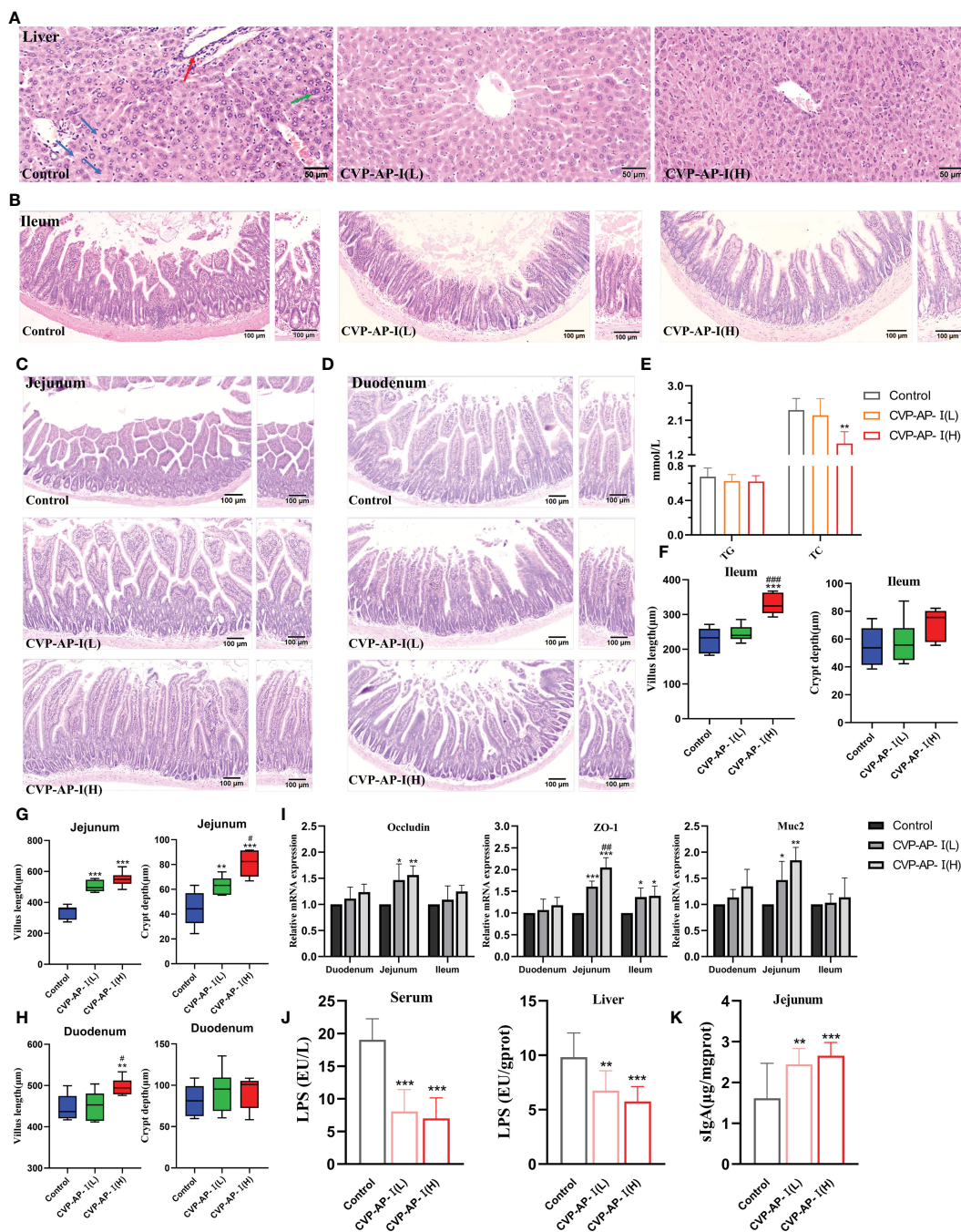
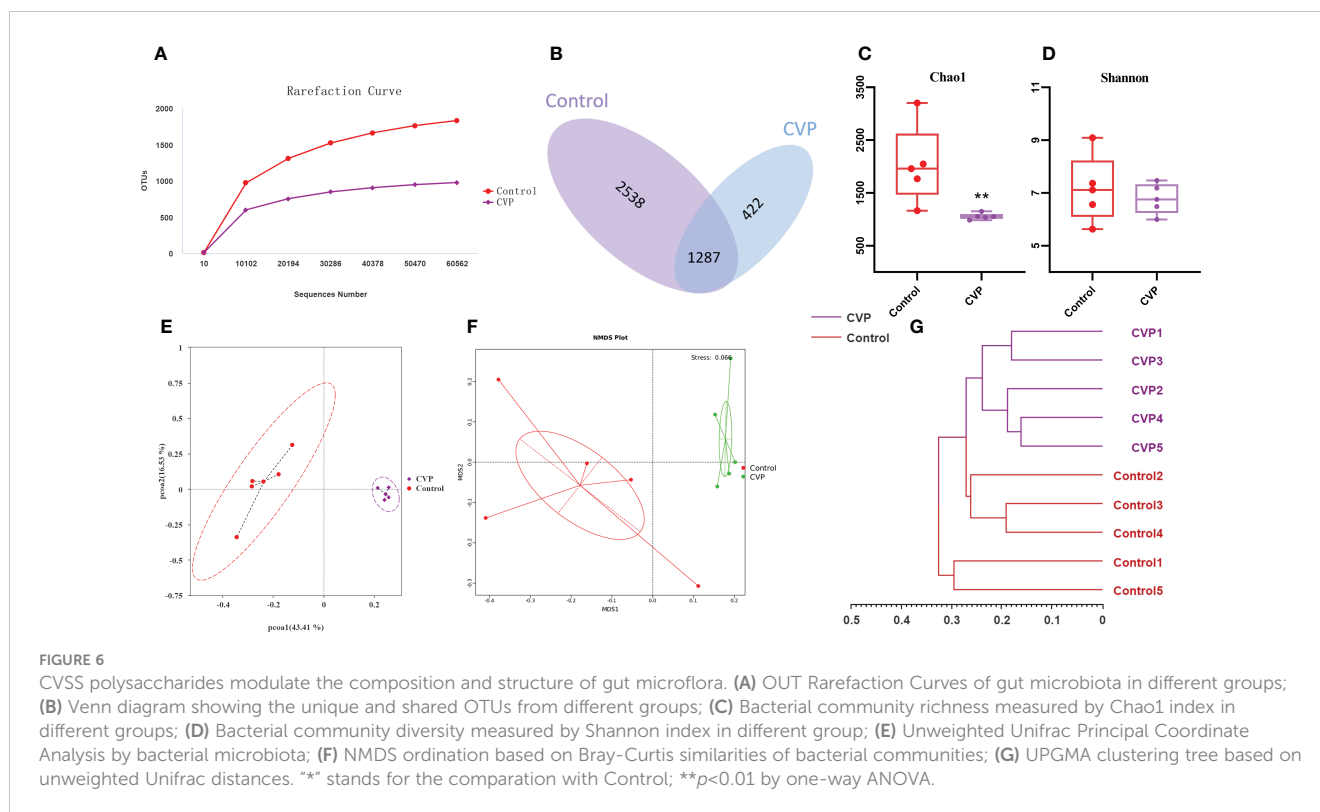


FIGURE 5

Effects of CVP-AP-I on liver and intestinal histology and intestinal immune barrier in naturally aging mice. (A) Representative images of H.E staining show that CVP-AP-I improves age-induced liver lesions. (“→” Inflammatory cell necrosis of the liver; “→” Multinucleated hepatocytes; “→” Mild steatosis of hepatocytes); (B–D) Representative images of H.E staining show that CVP-AP-I reverses aging-induced villus and crypt defects in the ileum, jejunum and duodenum; (E) Quantification shows the levels of TG and TC in the serum of different groups of mice (n=4); (F–H) Quantitative show of CVP reversal of aging-induced intestinal villus and crypt defects in the ileum, jejunum and duodenum. Error bars indicate Mix to Max (n = 6); (I) qRT-PCR results show the expressions of Occludin, ZO-1 and Muc2 in duodenum, jejunum and ileum of mice from different groups (n=4); (J) Quantification shows LPS levels in the serum and liver of different groups of mice (n=4); (K) Quantification shows sIgA levels in the jejunum of different groups of mice (n=6). All data are expressed as mean ± SD. **p*<0.05, ***p*<0.01, and ****p*<0.001 as compared with Control Group. #*p*<0.05, ##*p*<0.01, and ###*p*<0.001 as compared with CVP-AP-I(L) group.

distance-based Principal Co-ordinate analysis (PCOA) (71), Bray-Curtis distance-based metric-free multidimensional calibration method analysis (NMDS) (72) and UPGMA cluster analysis (73) were performed. We found that the CVP group was completely

separated from the control group in both the PCoA and NMDS analyses (Figures 6E, F), and the community composition of the samples was more similar. Similarly, in the UPGMA cluster tree analysis, we found that samples from the polysaccharide group

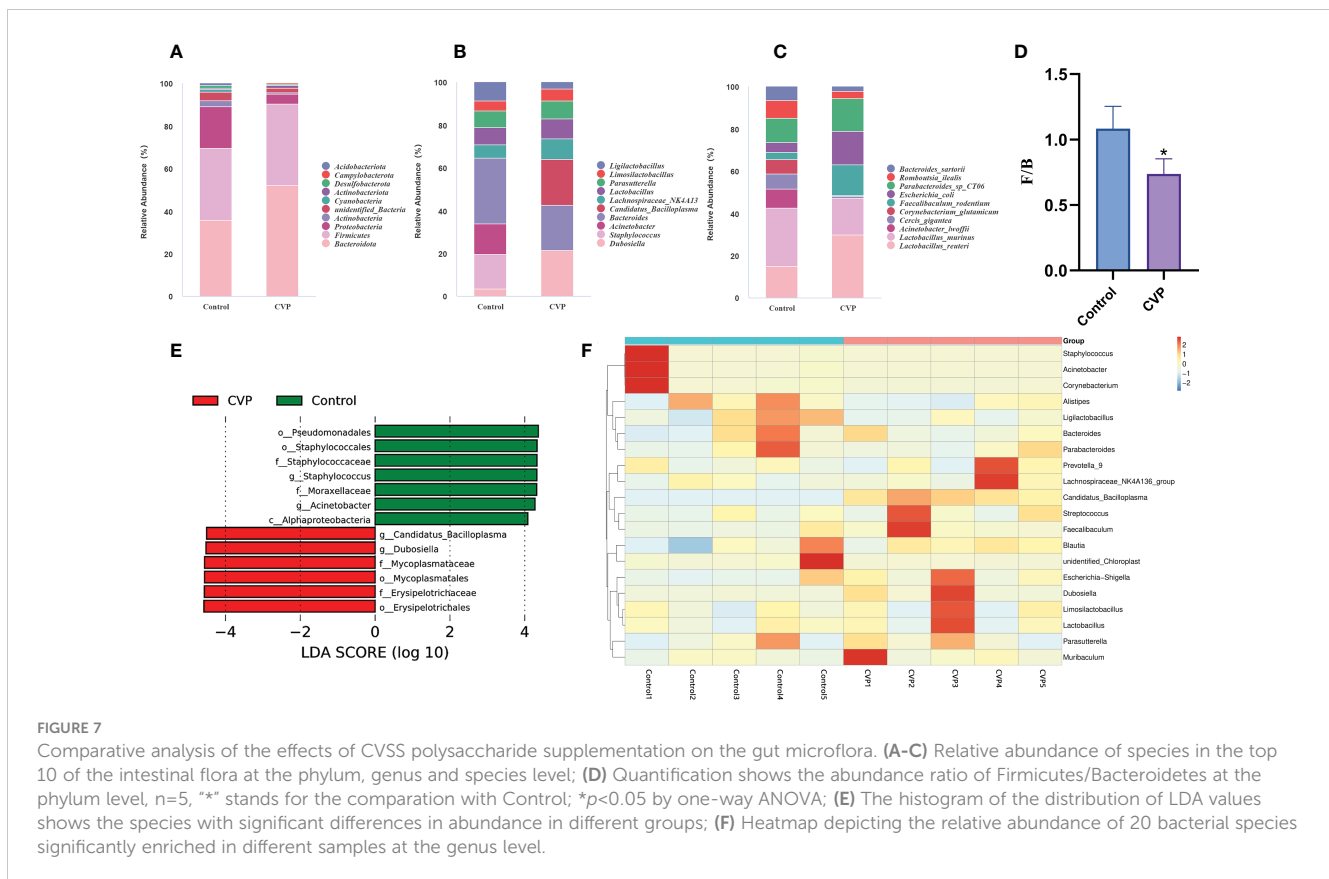


tended to cluster together, while samples from the control group were scattered or clustered (Figure 6G).

Furthermore, we studied the taxonomic distribution of abundant bacteria at three levels: phylum, genus and species. At the phylum level (Figure 7A), the control group was mainly composed of *Bacteroidota* (33.80%), *Firmicutes* (32.07%), *Proteobacteria* (18.45%), *unidentified_Bacteria* (3.58%) and *Actinobacteria* (2.86%), while the CVP group consisted of *Bacteroidota* (50.25%), *Firmicutes* (36.64%), *Proteobacteria* (4.69%), *unidentified_Bacteria* (2.11%), and *Actinobacteriota* (1.33%). Studies have shown that phylum horizontal *actinomycetes*, *Proteobacteria* and *Verrucomicrobia* increased significantly and *Firmicutes* decreased during aging (74, 75). However, CVSS polysaccharide could reverse this phenomenon, and the abundance of *Bacteroidetes* ($p < 0.01$) and *Firmicutes* ($p > 0.05$) in our polysaccharide group increased, while the abundance of *Proteobacteria* ($p < 0.01$) and *actinomycetes* ($p > 0.05$) decreased. We then calculated the abundance ratio of *Firmicutes/Bacteroidetes* (Figure 7D), which tended to increase with age and has been suggested as a possible marker of senescence (76). The abundance ratio of *Firmicutes/Bacteroidetes* significantly decreased in CVP group ($p = 0.023$). The analysis of the relative abundance of microbes at the genus level is shown in Figure 7B. *Bacteroides* (7.63%) was the most enriched genera in Control group, followed by *Staphylococcus* (3.96%), *Acinetobacter* (3.52%), *Lactobacillus* (1.97%), *Parasutterella* (1.90%), *Lactobacillus* (1.97%) and *Lachnospiraceae_NK4A136_group* (1.53%). *Dubosiella* (6.29%) and *Bacteroides* (6.27%) were the most abundant genera in the CVP group, followed by *Candidatus_Bacilloplasma* (5.38%), *Lachnospiraceae_NK4A136_group* (2.84%), *Lactobacillus* (2.75%) and *Parasutterella* (2.42%). At the species level, we observed higher relative

abundance of *Lactobacillus_reuteri* and *Faecalibaculum_rodentium* and lower relative abundance of *Acinetobacter_lwoffii*, *Cercis_gigantea*, and *Corynebacterium_glutamicum* in the CVP group compared to the control group (Figure 7C). In addition to *Dubosiella* and *Candidatus_Bacilloplasma*, which increased significantly in the CVP group at the genus level, there were also some increases in the abundance of the genera *Lactobacillus* and *Parasutterella*. Of these, *Lactobacillus* was widely used as one of the most common probiotics (77). Our results showed that *Lactobacillus_reuteri* was the most abundant at the species level in the genus *Lactobacillus*, which protected the micro-ecological balance of the gut by producing reuterin, short-chain fatty acids (SCFA), and lactic acid (78). In addition, *Parasutterella* has been shown to be involved in the maintenance of bile acid homeostasis and cholesterol metabolism (79). All these data indicate that CVSS polysaccharide can regulate the composition and structure of intestinal microorganisms.

To identify key phylotypes of the gut microbiota associated with CVSS polysaccharide function, we used linear discriminant analysis (LDA) to assess cecum microbes in the control and CVP groups. Figure 7E shows species with significant differences, indicated by LDA scores > 4.0 , reflecting the degree of impact of species that differed significantly between the two groups. At the genus level, the CVP group significantly increased the abundance of *Dubosiella* and *Candidatus_Bacilloplasma* and significantly decreased the abundance of *Staphylococcus* and *Acinetobacter*. *Dubosiella* is isolated and cultured from mouse intestinal contents (80) but there are few studies on its efficacy. It has been reported that *Dubosiella* significantly improves the state of dysglycemia and lipid metabolism in mice and prolongs the life span of nematodes. Surprisingly, in the treatment of high-fat diet-



induced obesity (81), alcoholic fatty liver (82), and inflammatory bowel disease (83) with polysaccharides, the abundance of *Dubosiella* was also increased, in the same way as our results, and in some cases predominantly. To further analyse the differences in species abundance, a heat map was generated using the top twenty bacteria in abundance at the genus level for species composition analysis. We found that 19 genera changed in the CVP group compared to the control group, with a trend towards enrichment in 11 genera and a decrease in abundance in 8 genera (Figure 7F). Among the genera with increased abundance, *Dubosiella* (80, 84), *Candidatus_Bacilloplasma* (85), *Lachnospiraceae_NK4A136_group* (86), *Faecalibaculum* (87), *Limosilactobacillus* (88, 89), *Lactobacillus* (77) and *Parasutterella* (79) were associated with intestinal homeostasis. Some of the genera with reduced abundance were associated with intestinal inflammation and oxidative stress, such as *Staphylococcus* (90, 91), *Acinetobacter* (92, 93), *Corynebacterium* (94, 95). Therefore, CVSS polysaccharide may regulate the homeostasis of the intestinal flora by increasing the abundance of potentially beneficial bacteria such as *Dubosiella* and *Candidatus_Bacilloplasma*, as well as common beneficial bacteria such as *Lactobacillus*, *Lactobacillus_reuteri* and *Parasutterella*, and decreasing the abundance of harmful bacteria such as *Staphylococcus* and *Fusobacterium*, thereby protecting the normal function of the intestine.

Finally, we performed a heatmap correlation analysis using the top ten abundances of intestinal microorganisms at the genus level with pro-inflammatory factors, antioxidant enzymes, MDA, LPS and sIgA in serum (Figure 8A), jejunum (Figure 8B) and liver (Figure 8C). We found that *Dubosiella*, *Candidatus_Bacilloplasma*,

Lachnospiraceae_NK4A136_group, *Lactobacillus*, *Parasutterella*, and *Limosilactobacillus* were negatively correlated with the levels of pro-inflammatory factors (IL-6, IL-1 β , TNF- α), LPS (serum), and MDA in serum, jejunum, and liver, and positively correlated with the levels of antioxidant enzymes (CAT, SOD, GPX) and sIgA (jejunum). *Staphylococcus*, *Acinetobacter*, and *Ligilactobacillus* were positively correlated with the levels of pro-inflammatory factors (IL-6, IL-1 β , TNF- α), LPS (serum), and MDA in serum, jejunum, and liver, and negatively correlated with the levels of antioxidant enzymes (CAT, SOD, GPX) and sIgA (jejunum). Seven of the top ten genera in abundance were significantly correlated with inflammatory, oxidative, and other factors, which further verified the above speculated that intestinal flora alleviated oxidative stress and inflammatory response and delayed aging through the gut-liver axis. As shown in Figure 9, during the aging process, under the action of ROS, the intestine and liver were damaged by oxidative stress, the intestinal barrier was damaged, the intestinal flora was disturbed, and inflammation was triggered. LPS produced by Gram-negative bacteria and metabolites produced by other microorganisms, and inflammatory factors entered the liver through the intestinal epithelial layer through the portal vein, aggravating the oxidative stress damage in the liver. By promoting the expression of transcription factor Nrf2, CVSS polysaccharide enhanced antioxidant capacity, reduced inflammatory response, repaired intestinal immune damage and regulated dysbiosis, thereby improving oxidative stress damage and inflammatory response in the intestine and liver of naturally aging mice through the intestine-liver axis. The protective effects on the

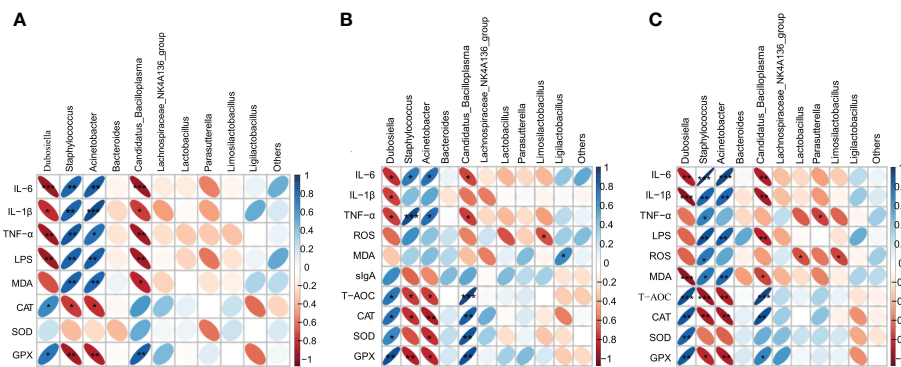


FIGURE 8 Heatmap showing the correlation of gut microbial genera with pro-inflammatory factors (IL-6, IL-1β, TNF-α), antioxidant enzymes (CAT, SOD, GPX), MDA, LPS, sIgA; (A) indicates correlation with serum; (B) indicates correlation with jejunum; (C) indicates correlation with liver. The colour and shape of the ellipse correlates with the strength of the correlation, with darker and flatter ellipses being more strongly correlated (* $p < 0.05$, ** $p < 0.01$, *** $p < 0.001$).

intestine and liver exhibited by the polysaccharide from the stems and leaves of *Chuanminshen violaceum* indicated that the polysaccharides from the stems and leaves had the same good pharmacological activity as the polysaccharides from the medicinal parts of the root, suggesting a predictable application *in vivo* against oxidative stress-related intestinal and liver diseases. In order to further develop and utilize the non-medicinal parts of the ground, more in-depth research is needed.

4 Conclusion

In this study, we used DEAE anion-exchange chromatography and gel filtration to obtain a homogeneous acidic polysaccharide, CVP-AP-I, from the stems and leaves of *Chuanminshen violaceum*. The results of chemical composition studies showed that CVP-AP-I is mainly composed of GalA, Gal, Ara, and Rha, and its average molecular

weight is 118.2kDa. Subsequently, different doses of CVP-AP-I were orally administered to naturally aging mice, and benefits in terms of oxidative stress and inflammation in the intestine and liver were reported. CVP-AP-I not only improved intestinal function by down-regulating ROS levels and pro-inflammatory factor expression, up-regulating antioxidant enzymes and total antioxidant capacity, repairing structural damage to intestinal tissues and modulating intestinal flora structure, but also has the same effect in liver tissue. These results suggest that CVSS Polysaccharide is an effective modulator and contributes to the homeostasis of the intestinal microbiota and its associated intestinal functions. With improved intestinal flora and intestinal immune barrier, LPS-producing Gram-negative bacteria such as *Acinetobacter* decrease, *Lactobacillus reuteri*, *Parasutterella*, and possibly the potentially beneficial bacterium *Dubosiaella* increase. CVSS polysaccharide reduces serum and hepatic LPS levels, thereby improving oxidative stress and inflammatory responses in the gut and liver through the gut-liver axis.

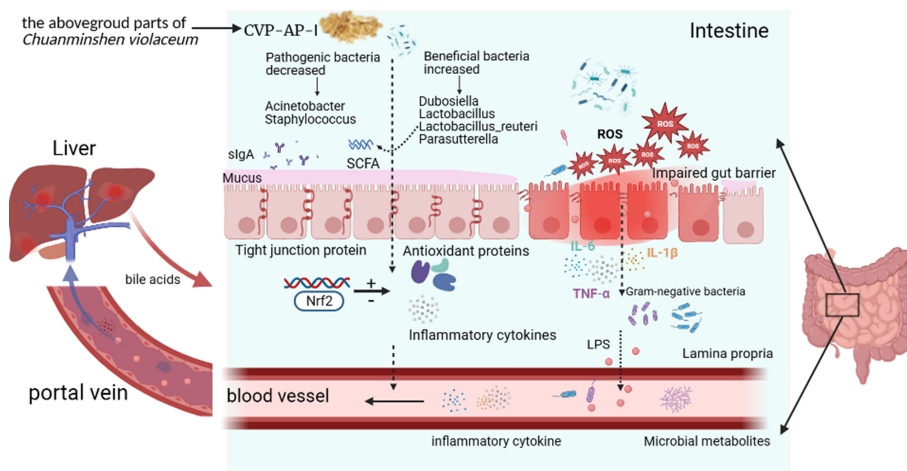


FIGURE 9 Summary diagram of the pharmacological effects of CVP-AP-I.

Data availability statement

The datasets presented in this study can be found in online repositories. The names of the repository/repositories and accession number(s) can be found below: NCBI Bioproject, PRJNA936077.

Ethics statement

The animal study was reviewed and approved by the Animal Care and Use Committee guidelines of Sichuan Agricultural University.

Author contributions

Y-FZ and X-PJ designed the study, C-YL, X-PJ, Y-PF, C-WZ and N-YL finished the experiment; X-PJ drafted the manuscript. L-XL, Z-QY and XS were mainly responsible for the determination of characterization of polysaccharides. X-HZ, H-QT, JC, Y-PL and X-FC detected the bioactivity of polysaccharides. BF and GY performed the graphics and helped to improve the research. Y-FZ, M-LT guided the experiments and reviewed the manuscript. All authors contributed to the article and approved the submitted version.

References

- Zinger A, Cho WC, Ben-Yehuda A. Cancer and aging - the inflammatory connection. *Aging Dis* (2017) 8:611–27. doi: 10.14336/AD.2016.1230
- Jeon SG, Song EJ, Lee D, Park J, Nam Y, Kim JI, et al. Traditional oriental medicines and alzheimer's disease. *Aging Dis* (2019) 10:307–28. doi: 10.14336/AD.2018.0328
- Hu C, Zhang X, Teng T, Ma ZG, Tang QZ. Cellular senescence in cardiovascular diseases: a systematic review. *Aging Dis* (2022) 13:103–28. doi: 10.14336/AD.2021.0927
- Harman D. Aging: a theory based on free radical and radiation chemistry. *J Gerontol* (1956) 11:298–300. doi: 10.1093/geronj/11.3.298
- Szilard L. On the nature of the aging process. *Proc Natl Acad Sci U S A* (1959) 45:30–45. doi: 10.1073/pnas.45.1.30
- Vatner SF, Zhang J, Oydanich M, Berkman T, Naftalovich R, Vatner DE. Healthful aging mediated by inhibition of oxidative stress. *Ageing Res Rev* (2020) 64:101194. doi: 10.1016/j.arr.2020.101194
- De Martinis M, Franceschi C, Monti D, Ginaldi L. Inflamm-aging and lifelong antigenic load as major determinants of ageing rate and longevity. *FEBS Lett* (2005) 579:2035–9. doi: 10.1016/j.febslet.2005.02.055
- Fougère B, Boulanger E, Nourhashemi F, Guyonnet S, Cesari M. Chronic inflammation: accelerator of biological aging. *J Gerontol Biol Sci Med Sci* (2017) 72:1218–25. doi: 10.1093/gerona/glw240
- Soenen S, Rayner CK, Jones KL, Horowitz M. The ageing gastrointestinal tract. *Curr Opin Clin Nutr Metab Care* (2016) 19:12–8. doi: 10.1097/MCO.0000000000000238
- Kim M, Benayoun BA. The microbiome: an emerging key player in aging and longevity. *Transl Med Aging* (2020) 4:103–16. doi: 10.1016/j.tma.2020.07.004
- Tarao K, So K, Moroi T, Ikeuchi T, Suyama T. Detection of endotoxin in plasma and ascitic fluid of patients with cirrhosis: its clinical significance. *Gastroenterology* (1977) 73:539–42. doi: 10.1016/S0016-5085(19)32137-7
- Triger DR, Boyer TD, Levin J. Portal and systemic bacteraemia and endotoxaemia in liver disease. *Gut* (1978) 19:935–9. doi: 10.1136/gut.19.10.935
- Wahlström A, Sayin SI, Marschall HU, Bäckhed F. Intestinal crosstalk between bile acids and microbiota and its impact on host metabolism. *Cell Metab* (2016) 24:41–50. doi: 10.1016/j.cmet.2016.05.005
- Perino A, Demagny H, Velazquez-Villegas L, Schoonjans K. Molecular physiology of bile acid signaling in health, disease, and aging. *Physiol Rev* (2021) 101:683–731. doi: 10.1152/physrev.00049.2019

Acknowledgments

We acknowledge the support by the Natural Medicine Research Center, College of Veterinary Medicine of Sichuan Agricultural University for providing the experimental site and relevant experimental instruments.

Conflict of interest

The authors declare that the research was conducted in the absence of any commercial or financial relationships that could be construed as a potential conflict of interest.

Publisher's note

All claims expressed in this article are solely those of the authors and do not necessarily represent those of their affiliated organizations, or those of the publisher, the editors and the reviewers. Any product that may be evaluated in this article, or claim that may be made by its manufacturer, is not guaranteed or endorsed by the publisher.

- Marshall JC. The gut as a potential trigger of exercise-induced inflammatory responses. *Can J Physiol Pharmacol* (1998) 76:479–84. doi: 10.1139/cjpp-76-5-479
- Milosevic I, Vujovic A, Barac A, Djelic M, Korac M, Radovanovic SA, et al. Gut-liver axis, gut microbiota, and its modulation in the management of liver diseases: a review of the literature. *Int J Mol Sci* (2019) 20(2):395. doi: 10.3390/ijms20020395
- Albillos A, de Gottardi A, Rescigno M. The gut-liver axis in liver disease: pathophysiological basis for therapy. *J Hepatol* (2020) 72:558–77. doi: 10.1016/j.jhep.2019.10.003
- Bajaj JS, Heuman DM, Hylemon PB, Sanyal AJ, White MB, Monteith P, et al. Altered profile of human gut microbiome is associated with cirrhosis and its complications. *J Hepatol* (2014) 60:940–7. doi: 10.1016/j.jhep.2013.12.019
- Boursier J, Mueller O, Barret M, Machado M, Fizanne L, Araujo-Perez F, et al. The severity of nonalcoholic fatty liver disease is associated with gut dysbiosis and shift in the metabolic function of the gut microbiota. *Hepatology* (2016) 63:764–75. doi: 10.1002/hep.28356
- Vaiserman AM, Koliada AK, Marotta F. Gut microbiota: a player in aging and a target for anti-aging intervention. *Ageing Res Rev* (2017) 35:36–45. doi: 10.1016/j.arr.2017.01.001
- Dong H, Zhang Q, Li L, Liu J, Shen L, Li H, et al. Antioxidant activity and chemical compositions of essential oil and ethanol extract of chuanminshen violaceum. *Ind Crops Prod* (2015) 76:290–7. doi: 10.1016/j.indcrop.2015.04.051
- Yu Y, Shen M, Song Q, Xie J. Biological activities and pharmaceutical applications of polysaccharide from natural resources: a review. *Carbohydr Polym* (2018) 183:91–101. doi: 10.1016/j.carbpol.2017.12.009
- Fan J, Feng H, Yu Y, Sun M, Liu Y, Li T, et al. Antioxidant activities of the polysaccharides of chuanminshen violaceum. *Carbohydr Polym* (2017) 157:629–36. doi: 10.1016/j.carbpol.2016.10.040
- Zhao X, Zhang Y, Song X, Yin Z, Jia R, Zhao X, et al. Effect of chuanminshen violaceum polysaccharides and its sulfated derivatives on immunosuppression induced by cyclophosphamide in mice. *Int J Clin Exp Med* (2015) 8:558–68. Available at: <https://pubmed.ncbi.nlm.nih.gov/25785030/>
- Song X, Yin Z, Zhao X, Cheng A, Jia R, Yuan G, et al. Antiviral activity of sulfated chuanminshen violaceum polysaccharide against newcastle disease virus. *J Gen Virol* (2013) 94:2164–74. doi: 10.1099/vir.0.054270-0
- Huang C, Li ZX, Wu Y, Huang ZY, Hu Y, Gao J. Treatment and bioresources utilization of traditional chinese medicinal herb residues: recent technological advances and industrial prospect. *J Environ Manage* (2021) 299:113607. doi: 10.1016/j.jenvman.2021.113607

27. Wang H, Peng D, Xie J. Ginseng leaf-stem: bioactive constituents and pharmacological functions. *Chin Med* (2009) 4:20. doi: 10.1186/1749-8546-4-20
28. Liu B, Shang ZZ, Li QM, Zha XQ, Wu DL, Yu NJ, et al. Structural features and anti-gastric cancer activity of polysaccharides from stem, root, leaf and flower of cultivated dendrobium huoshanense. *Int J Biol Macromol* (2020) 143:651–64. doi: 10.1016/j.ijbiomac.2019.12.041
29. Feng H, Fan J, Qiu H, Wang Z, Yan Z, Yuan L, et al. Chuanminshen violaceum polysaccharides improve the immune responses of foot-and-mouth disease vaccine in mice. *Int J Biol Macromol* (2015) 78:405–16. doi: 10.1016/j.ijbiomac.2015.04.044
30. DuBois M, Gilles KA, Hamilton JK, Rebers PA, Smith F. Colorimetric method for determination of sugars and related substances. *Anal Chem* (1956) 28:350–6. doi: 10.1021/ac60111a017
31. Huang C, Peng X, Pang DJ, Li J, Paulsen BS, Rise F, et al. Pectic polysaccharide from nelumbo nucifera leaves promotes intestinal antioxidant defense *in vitro* and *in vivo*. *Food Funct* (2021) 12:10828–41. doi: 10.1039/d1fo02354c
32. Singleton VL, Rossi JA. Colorimetry of total phenolics with phosphomolybdic-phosphotungstic acid reagents. *Am J Enol Vitic* (1965) 16:144. Available at: <https://www.ajeonline.org/content/16/3/144>
33. Bradford MM. A rapid and sensitive method for the quantitation of microgram quantities of protein utilizing the principle of protein-dye binding. *Anal Biochem* (1976) 72:248–54. doi: 10.1006/abio.1976.9999
34. Zou YF, Li CY, Fu YP, Jiang QX, Peng X, Li LX, et al. The comparison of preliminary structure and intestinal anti-inflammatory and anti-oxidative activities of polysaccharides from different root parts of angelica sinensis (oliv.) diels. *J Ethnopharmacol* (2022) 295:115446. doi: 10.1016/j.jep.2022.115446
35. Zou Y, Zhang Y, Paulsen BS, Rise F, Chen Z, Jia R, et al. New pectic polysaccharides from codonopsis pilosula and codonopsis tangshen: structural characterization and cellular antioxidant activities. *J Sci Food Agric* (2021) 101:6043–52. doi: 10.1002/jsfa.11261
36. Lin S, Li HY, Wang ZY, Liu X, Yang Y, Cao ZW, et al. Analysis of methanolic extracts and crude polysaccharides from the leaves of chuanminshen violaceum and their antioxidant activities. *Antioxidants (Basel)* (2019) 8(8):266. doi: 10.3390/antiox8080266
37. Dong H, Zhang Q, Li Y, Li L, Lan W, He J, et al. Extraction, characterization and antioxidant activities of polysaccharides of chuanminshen violaceum. *Int J Biol Macromol* (2016) 86:224–32. doi: 10.1016/j.ijbiomac.2016.01.002
38. Sohal RS, Orr WC. The redox stress hypothesis of aging. *Free Radic Biol Med* (2012) 52:539–55. doi: 10.1016/j.freeradbiomed.2011.10.445
39. Sen P, Shah PP, Nativo R, Berger SL. Epigenetic mechanisms of longevity and aging. *Cell* (2016) 166:822–39. doi: 10.1016/j.cell.2016.07.050
40. Sookoian S, Pirola CJ. Liver enzymes, metabolomics and genome-wide association studies: from systems biology to the personalized medicine. *World J Gastroenterol* (2015) 21:711–25. doi: 10.3748/wjg
41. Li XT, Zhang YK, Kuang HX, Jin FX, Liu DW, Gao MB, et al. Mitochondrial protection and anti-aging activity of astragalus polysaccharides and their potential mechanism. *Int J Mol Sci* (2012) 13:1747–61. doi: 10.3390/ijms13021747
42. Saffrey MJ. Aging of the mammalian gastrointestinal tract: a complex organ system. *Age (Dordr)* (2014) 36:9603. doi: 10.1007/s11357-013-9603-2
43. Cockburn DW, Koropatkin NM. Polysaccharide degradation by the intestinal microbiota and its influence on human health and disease. *J Mol Biol* (2016) 428:3230–52. doi: 10.1016/j.jmb.2016.06.021
44. Zou YF, Li CY, Fu YP, Feng X, Peng X, Feng B, et al. Restorative effects of inulin from codonopsis pilosula on intestinal mucosal immunity, anti-inflammatory activity and gut microbiota of immunosuppressed mice. *Front Pharmacol* (2022) 13:786141. doi: 10.3389/fphar.2022.786141
45. Sun Z, Zhang S, Chan JY, Zhang DD. Keap1 controls postinduction repression of the nrf2-mediated antioxidant response by escorting nuclear export of nrf2. *Mol Cell Biol* (2007) 27:6334–49. doi: 10.1128/MCB.00630-07
46. Taguchi K, Motohashi H, Yamamoto M. Molecular mechanisms of the keap1–nrf2 pathway in stress response and cancer evolution. *Genes Cells* (2011) 16:123–40. doi: 10.1111/j.1365-2443.2010.01473
47. Li Y, Chen X, Zhang H, Xiao J, Yang C, Chen W, et al. 4-octyl itaconate alleviates lipopolysaccharide-induced acute lung injury in mice by inhibiting oxidative stress and inflammation. *Drug Des Devel Ther* (2020) 14:5547–58. doi: 10.2147/DDDT.S280922
48. Saha S, Buttari B, Panieri E, Profumo E, Saso L. An overview of nrf2 signaling pathway and its role in inflammation. *Molecules* (2020) 25(22):5474. doi: 10.3390/molecules25225474
49. Zhao Y, Sun Y, Wang G, Ge S, Liu H. Dendrobium officinale polysaccharides protect against mnng-induced plgc in rats via activating the nrf2 and antioxidant enzymes ho-1 and nqo-1. *Oxid Med Cell Longev* (2019) 2019:9310245. doi: 10.1155/2019/9310245
50. Xing YY, Zheng YK, Yang S, Zhang LH, Guo SW, Shi LL, et al. Artemisia ordosica polysaccharide alleviated lipopolysaccharide-induced oxidative stress of broilers via nrf2/keap1 and tlr4/nf-kb pathway. *Ecotoxicol Environ Saf* (2021) 223:112566. doi: 10.1016/j.ecoenv.2021.112566
51. Davalli P, Mitic T, Caporali A, Lauriola A, D'Arca D. Ros, cell senescence, and novel molecular mechanisms in aging and age-related diseases. *Oxid Med Cell Longev* (2016) 2016:3565127. doi: 10.1155/2016/3565127
52. Kim MJ, Kim DH, Bang E, Noh SG, Chun P, Yokozawa T, et al. Ppar α agonist, mhy3200, alleviates renal inflammation during aging via regulating ros/akt/foxo1 signaling. *Molecules* (2021) 26(11):3197. doi: 10.3390/molecules26113197
53. Romero FJ, Bosch-Morell F, Romero MJ, Jareño EJ, Romero B, Marin N, et al. Lipid peroxidation products and antioxidants in human disease. *Environ Health Perspect* (1998) 106 Suppl 5:1229–34. doi: 10.1289/ehp.98106s51229
54. Huang Y, Chen H, Zhang K, Lu Y, Wu Q, Chen J, et al. Extraction, purification, structural characterization, and gut microbiota relationship of polysaccharides: a review. *Int J Biol Macromol* (2022) 213:967–86. doi: 10.1016/j.ijbiomac.2022.06.049
55. Shenghua P, Ziqin Z, Shuyu T, Huixia Z, Xianglu R, Jiao G. An integrated fecal microbiome and metabolome in the aged mice reveal anti-aging effects from the intestines and biochemical mechanism of fufang zhenshu tiaozhi(ftz). *BioMed Pharmacother* (2020) 121:109421. doi: 10.1016/j.biopha.2019.109421
56. Wang Z, Xu M, Peng J, Jiang L, Hu Z, Wang H, et al. Prevalence and associated metabolic factors of fatty liver disease in the elderly. *Exp Gerontol* (2013) 48:705–9. doi: 10.1016/j.exger.2013.05.059
57. Kim IH, Kisseleva T, Brenner DA. Aging and liver disease. *Curr Opin Gastroenterol* (2015) 31:184–91. doi: 10.1097/MOG.0000000000000176
58. Agarwal A, Saleh RA, Bedaiwy MA. Role of reactive oxygen species in the pathophysiology of human reproduction. *Fertil Steril* (2003) 79:829–43. doi: 10.1016/s0015-0282(02)04948-8
59. Capaldo CT, Powell DN, Kalman D. Layered defense: how mucus and tight junctions seal the intestinal barrier. *J Mol Med (Berl)* (2017) 95:927–34. doi: 10.1007/s00109-017-1557-x
60. Guerbet T, Boudry G, Lan A. Mitochondrial function in intestinal epithelium homeostasis and modulation in diet-induced obesity. *Mol Metab* (2022) 63:101546. doi: 10.1016/j.molmet.2022.101546
61. Turner JR. Intestinal mucosal barrier function in health and disease. *Nat Rev Immunol* (2009) 9:799–809. doi: 10.1038/nri2653
62. Lai Z, Lin L, Zhang J, Mao S. Effects of high-grain diet feeding on mucosa-associated bacterial community and gene expression of tight junction proteins and inflammatory cytokines in the small intestine of dairy cattle. *J Dairy Sci* (2022) 105:6601–15. doi: 10.3168/jds.2021-21355
63. Katz D, Hollander D, Said HM, Dadufalza V. Aging-associated increase in intestinal permeability to polyethylene glycol 900. *Dig Dis Sci* (1987) 32:285–8. doi: 10.1007/BF01297055
64. Ma TY, Hollander D, Dadufalza V, Krugliak P. Effect of aging and caloric restriction on intestinal permeability. *Exp Gerontol* (1992) 27:321–33. doi: 10.1016/0531-5565(92)90059-9
65. Hooper LV, Littman DR, Macpherson AJ. Interactions between the microbiota and the immune system. *Science* (2012) 336:1268–73. doi: 10.1126/science.1223490
66. Yang XW, Wang N, Li W, Xu W, Wu S. Biotransformation of 4,5-o-dicaffeoylquinic acid methyl ester by human intestinal flora and evaluation on their inhibition of no production and antioxidant activity of the products. *Food Chem Toxicol* (2013) 55:297–303. doi: 10.1016/j.fct.2012.12.039
67. Ma Z, Zhang F, Ma H, Chen X, Yang J, Yang Y, et al. Effects of different types and doses of whey protein on the physiological and intestinal flora in d-galactose induced aging mice. *PLoS One* (2021) 16:e248329. doi: 10.1371/journal.pone.0248329
68. Song C, Zhang Y, Cheng L, Shi M, Li X, Zhang L, et al. Tea polyphenols ameliorates memory decline in aging model rats by inhibiting brain tlr4/nf-kb inflammatory signaling pathway caused by intestinal flora dysbiosis. *Exp Gerontol* (2021) 153:111476. doi: 10.1016/j.exger.2021.111476
69. Lundberg DS, Yourstone S, Mieczkowski P, Jones CD, Dangl JL. Practical innovations for high-throughput amplicon sequencing. *Nat Methods* (2013) 10:999–1002. doi: 10.1038/nmeth.2634
70. Li B, Zhang X, Guo F, Wu W, Zhang T. Characterization of tetracycline resistant bacterial community in saline activated sludge using batch stress incubation with high-throughput sequencing analysis. *Water Res* (2013) 47:4207–16. doi: 10.1016/j.watres.2013.04.021
71. Equbal J, Lakra RK, Savurirajan M, Satyam K, Thiruchitrabalam G. Assessing the benthic quality status of three fine sand tropical beaches from the andaman islands through the application of marine biotic indices. *Environ Monit Assess* (2022) 194:479. doi: 10.1007/s10661-022-10132-6
72. Krabbe PF, Salomon JA, Murray CJ. Quantification of health states with rank-based nonmetric multidimensional scaling. *Med Decis Mak* (2007) 27:395–405. doi: 10.1177/0272989X07302131
73. Lü J, Guo W, Chen S, Guo M, Qiu B, Yang C, et al. Host plants influence the composition of the gut bacteria in henosepilachna vigintioctopunctata. *PLoS One* (2019) 14:e224213. doi: 10.1371/journal.pone.0224213
74. Kang L, Li P, Wang D, Wang T, Hao D, Qu X. Alterations in intestinal microbiota diversity, composition, and function in patients with sarcopenia. *Sci Rep* (2021) 11:4628. doi: 10.1038/s41598-021-84031-0
75. Xu Y, Wang Y, Li H, Dai Y, Chen D, Wang M, et al. Altered fecal microbiota composition in older adults with frailty. *Front Cell Infect Microbiol* (2021) 11:696186. doi: 10.3389/fcimb.2021.696186
76. Vaiserman A, Romanenko M, Piven L, Moseiko V, Lushchak O, Kryzhanovska N, et al. Differences in the gut firmicutes to bacteroidetes ratio across age groups in

- healthy ukrainian population. *BMC Microbiol* (2020) 20:221. doi: 10.1186/s12866-020-01903-7
77. O'Callaghan J, O'Toole PW. Lactobacillus: host-microbe relationships. *Curr Top Microbiol Immunol* (2013) 358:119–54. doi: 10.1007/82_2011_187
78. Mu Q, Tavella VJ, Luo XM. Role of lactobacillus reuteri in human health and diseases. *Front Microbiol* (2018) 9:757. doi: 10.3389/fmicb.2018.00757
79. Ju T, Kong JY, Stothard P, Willing BP. Defining the role of parasutterella, a previously uncharacterized member of the core gut microbiota. *Isme J* (2019) 13:1520–34. doi: 10.1038/s41396-019-0364-5
80. Cox LM, Sohn J, Tyrrell KL, Citron DM, Lawson PA, Patel NB, et al. Corrigendum: description of two novel members of the family crysielotrichaceae: ileibacterium valens gen. nov., sp. nov. and dubosiella newyorkensis, gen. nov., sp. nov., from the murine intestine, and emendation to the description of faecalibacterium rodentium. *Int J Syst Evol Microbiol* (2017) 67:4289. doi: 10.1099/ijsem.0.002339
81. Lan Y, Sun Q, Ma Z, Peng J, Zhang M, Wang C, et al. Seabuckthorn polysaccharide ameliorates high-fat diet-induced obesity by gut microbiota-scfas-liver axis. *Food Funct* (2022) 13:2925–37. doi: 10.1039/d1fo03147c
82. Zhang Z, Chen X, Cui B. Modulation of the fecal microbiome and metabolome by resistant dextrin ameliorates hepatic steatosis and mitochondrial abnormalities in mice. *Food Funct* (2021) 12:4504–18. doi: 10.1039/d1fo00249j
83. Lai W, Wang C, Lai R, Peng X, Luo J. Lycium barbarum polysaccharide modulates gut microbiota to alleviate rheumatoid arthritis in a rat model. *NPJ Sci Food* (2022) 6:34. doi: 10.1038/s41538-022-00149-z
84. Yi Z, Liu X, Liang L, Wang G, Xiong Z, Zhang H, et al. Antrodin A from antrodia camphorata modulates the gut microbiome and liver metabolome in mice exposed to acute alcohol intake. *Food Funct* (2021) 12:2925–37. doi: 10.1039/d0fo03345f
85. Wei H, Wang H, Tang L, Mu C, Ye C, Chen L, et al. High-throughput sequencing reveals the core gut microbiota of the mud crab (*scylla paramamosain*) in different coastal regions of southern china. *BMC Genomics* (2019) 20:829. doi: 10.1186/s12864-019-6219-7
86. Ma L, Ni Y, Wang Z, Tu W, Ni L, Zhuge F, et al. Spermidine improves gut barrier integrity and gut microbiota function in diet-induced obese mice. *Gut Microbes* (2020) 12:1–19. doi: 10.1080/19490976.2020.1832857
87. Cao YG, Bae S, Villarreal J, Moy M, Chun E, Michaud M, et al. Faecalibaculum rodentium remodels retinoic acid signaling to govern eosinophil-dependent intestinal epithelial homeostasis. *Cell Host Microbe* (2022) 30:1295–310. doi: 10.1016/j.chom.2022.07.015
88. Wu Y, Ye Z, Feng P, Li R, Chen X, Tian X, et al. Limosilactobacillus fermentum jl-3 isolated from "jiangshui" ameliorates hyperuricemia by degrading uric acid. *Gut Microbes* (2021) 13:1–18. doi: 10.1080/19490976.2021.1897211
89. Oliveira LS, Wendt GW, Crestani A, Casaril K. The use of probiotics and prebiotics can enable the ingestion of dairy products by lactose intolerant individuals. *Clin Nutr* (2022) 41:2644–50. doi: 10.1016/j.clnu.2022.10.003
90. Liu J, Chen D, Peters BM, Li L, Li B, Xu Z, et al. Staphylococcal chromosomal cassettes mec (scmec): a mobile genetic element in methicillin-resistant staphylococcus aureus. *Microb Pathog* (2016) 101:56–67. doi: 10.1016/j.micpath.2016.10.028
91. Li Z, Dong J, Wang M, Yan J, Hu Y, Liu Y, et al. Resveratrol ameliorates liver fibrosis induced by nonpathogenic staphylococcus in balb/c mice through inhibiting its growth. *Mol Med* (2022) 28:52. doi: 10.1186/s10020-022-00463-y
92. Munoz-Price LS, Weinstein RA. Acinetobacter infection. *N Engl J Med* (2008) 358:1271–81. doi: 10.1056/NEJMra070741
93. Peleg AY, Seifert H, Paterson DL. Acinetobacter baumannii: emergence of a successful pathogen. *Clin Microbiol Rev* (2008) 21:538–82. doi: 10.1128/CMR.00058-07
94. Nasim F, Dey A, Qureshi IA. Comparative genome analysis of corynebacterium species: the underestimated pathogens with high virulence potential. *Infect Genet Evol* (2021) 93:104928. doi: 10.1016/j.meegid.2021.104928
95. Mangutov EO, Alieva AA, Kharseeva GG, Voronina NA, Alekseeva LP, Evdokimova VV, et al. Corynebacterium spp.: Relationship of pathogenic properties and antimicrobial resistance. *Klin Lab Diagn* (2022) 67:519–24. doi: 10.51620/0869-2084-2022-67-9-519-524